JOURNAL OF APPLIED ELECTROCHEMISTRY 18 (1988) 473–483

Current efficiency in aluminium reduction cells

Å. STERTEN

Institutt for teknisk elektrokjemi, NTH, Universitetet i Trondheim, N-7034 Trondheim-NTH, Norway

Received 7 July 1987; revised 21 November 1987

A simplified current efficiency model of the aluminium deposition reaction in sodium cryolitic melts was developed and discussed in view of literature data. The partial current density for aluminium production was derived to be

$$i_{Al} = Fk_{NaF}c_m[-1 + \exp(0.445\eta_{Al}/B)]$$

where k_{NaF} is the NaF mass transfer coefficient at the melt/metal interface and $B = -0.736$ V. η_{Al} is the concentration overvoltage for the aluminium deposition reaction. c_m is a modified concentration of NaF given by the equation

$$c_m/(\text{mol cm}^{-3}) = (x - 0.35)^{0.445}(1.030 - 0.687T/T_0)$$

where x is the molar fraction of NaF, while T/T_0 is a dimensionless temperature ratio with $T_0 = 1273$ K. The partial current density corresponding to the flux density of all reduced species being transported away from the metal/melt interface was derived to be

$$i_{loss} = Fk_{Na}c_{Na,eq}\left[-\alpha + \exp\left(-\frac{F}{RT}\eta_{Al}\right)\right]$$

where k_{Na} is a mixed mass transfer coefficient of reduced species in the boundary layer at the metal/melt surface, while α is the degree of saturation of Na(diss) related to the equilibrium value $c_{Na,eq}$. An empirical equation for $c_{Na,eq}$ as a function of temperature and melt composition was derived. The current efficiency of the aluminium deposition reaction is then

$$\varepsilon_{Al} = [i_{Al}/(i_{Al} + i_{loss})] - \varepsilon'_{Al}$$

where ε'_{Al} represents losses due to dispersed metal, aluminium carbide formation, sodium penetration into the carbon lining etc. The influences of various parameters on the mass transfer coefficients are briefly discussed.

1. Introduction

The current efficiency (CE) with respect to aluminium in industrial aluminium production cells normally ranges from 85 to 95%. The influence of various parameters on the CE is still controversial in spite of considerable research activity in the field. Literature reviews are given elsewhere [1, 2], and only papers of special interest in the present context will be cited. Normally, the cathodic CE is studied indirectly by analysis of the CO_2/CO ratio of the exit anode gases. However, the cathodic yield is most conveniently interpreted by the component fluxes across the aluminium/melt interface and related chemical reactions. Any interaction between the aluminium pool and the adjacent cell lining may, as a first approximation, be disregarded, since this type of metal loss should be treated as a separate problem. The present work reviews some recent data for metal solubility in the electrolyte [3] and discusses some kinetic aspects of the cathode process. This approach is a key to an improved understanding of the relationship between the aluminium deposition reaction, the back reactions, cathodic overvoltage and the corresponding concentration gradients in the boundary layers. Finally, this treatment makes it possible to derive the partial current densities, i_{Al} and i_{loss}, as a function of melt composition, temperature, overvoltage and the corresponding mass transfer coefficients. It should be emphasized that the partial current densities, as usual for electrode reactions, are a function of the electrode overvoltage.

Since accurate thermodynamic data for molten $NaF–AlF_3$ mixtures [4] are available, it is reasonable to use this system as a reference base for the theoretical treatment given below. The influence of various additives such as Al_2O_3 and CaF_2 may also preferably be referred to the pure $NaF–AlF_3$ system.

2. Metal solubility and transport properties

Aluminium reacts to a certain degree with the $NaF–AlF_3$ melts. The most accurate data in this field are given in a recent work by Ødegård [3]. Quenched samples were treated with HCl and the amounts of H_2 evolved were determined in order to evaluate the equilibrium content of metal in each sample. Ødegård

0021-891X/88 $03.00 + .12

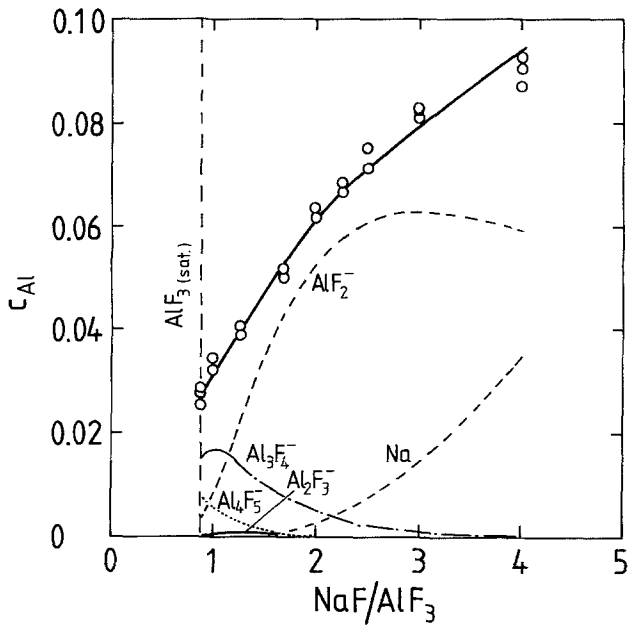

Fig. 1. Solubility of aluminium as wt % Al in a closed Al–NaF–AlF_3–Al_2O_3(sat) system as a function of the NaF/AlF_3 molar ratio. The partial solubilities of Na(diss), AlF_2^-, $Al_2F_3^-$, $Al_3F_4^-$ and $Al_4F_5^-$ are also included. Temperature 1273 K. From Ødegård [3].

presented several ionic models describing the nature of 'dissolved aluminium' in the system. These models were fitted to the experimental data by assuming proportionality between the concentration of reduced species and the activities of NaF and AlF_3 in agreement with the equilibrium reactions. Figure 1 shows the total solubility and the concentration of reduced entities predicted from Ødegård's favoured model. There is no doubt that aluminium is partly dissolved as Na(diss), the concentration of which increases with increasing basicity of the melt,

$$Al + 3NaF = AlF_3 + 3Na(diss) \quad (1)$$

The exact nature of Na(diss) is not completely clear, although it is fairly well established that the valence electron occupies some kind of anion vacancy surrounded by a certain number of cations [5]. In the binary NaF–Na(diss) system, where the concentration of dissolved sodium may be as high as $\simeq 1.1$ wt % at 1273 K [6], there is a certain electronic contribution to the total conductivity [7]. Adding AlF_3 to this system considerably reduces the equilibrium concentration of Na(diss), which means that the electronic contribution to the conductivity also drops. As discussed below the concentration of Na(diss) in the electrolyte of technical aluminium cells is far below the equilibrium concentration. It is easily estimated that the electronic contribution to the total conductivity in this case will be less than 1% and thus of minor importance. This conclusion is in agreement with a corresponding calculation performed by Ødegård [3].

The reduced entity having the highest concentration in moderately acidic melts is, apparently, AlF_2^-. However, even in this range of the system, Na(diss) may be even more important in the mass transfer of reduced entities across the boundary layers because of its electronic nature. According to Ødegård [3] the mean diffusion coefficient of all reduced species counted as Al(diss) in Na_3AlF_6 saturated with Al_2O_3 and Al at 1273 K is $\simeq 1 \times 10^{-4}$ cm^2 s^{-1}, which is roughly five times larger than the corresponding values for ordinary ions in molten salt systems.

An important parameter is the equilibrium concentration of Na(diss) in Reaction 1 with unit activity of aluminium. Using the model data of Ødegård [3] and density data of Paucirova *et al.* [8] the following empirical equation was derived,

$$c_{Na,eq}(\text{mol cm}^{-3}) = (1 - k_{Al_2O_3} - k_{Ad})k_T \times \exp(3x - 9.9)/x \quad (2)$$

where x is the molar fraction of NaF in the binary system NaF–AlF_3, while

$$k_T = 8\,423\,900 \exp(-20\,300/T) \quad (3)$$

is the temperature dependence of the solubility in the NaF–Na system as estimated from the work of Bredig and Bronstein [6]. $k_{Al_2O_3}$ and k_{Ad} are the individual effects of Al_2O_3 and other additives, respectively, on the equilibrium concentration of Na(diss). Numerical values for $k_{Al_2O_3}$ and k_{Ad} may be estimated from the work of Ødegård [3]. With zero additions we have $k_{Al_2O_3} \simeq k_{Ad} = 0$. The underlying assumption that the combined effect of various additives is the sum of the individual ones may of course be somewhat erroneous, but at present better data are not easily obtained.

The Na^+ ions carry the greater part of the electric current in cryolitic melts. In the NaF–AlF_3 system, saturated with alumina at 1300 K, the transference number is estimated to be 0.76 at the NaF/AlF_3 molar ratio $r = 10$ [9]. The transference number increases with increasing melt acidity and reaches a value of $t_{Na^+} = 0.99$ at the composition $r = 2.0$. The numerical values of the transference number are believed to be roughly independent of the alumina concentration.

For the sake of simplicity the transference number of Na^+ is taken to be unity for all melt compositions considered in the present work. The error thereby introduced is believed to be of minor importance.

3. The cathode process. Reaction mechanism

All stable reduced entities discussed above should be considered as final cathode products. However, for the sake of simplicity only Al, AlF_2^- and Na(diss), the most important species in basic and weakly acidic melts, will be dealt with.

A simple and logical reaction route for the aluminium formation reaction is proposed in Scheme 1.

Scheme 1:

(I) Migration of $3Na^+$ to the aluminium surface (3 Faradays).

(II) Diffusion of AlF_3 ($NaAlF_4$) to the aluminium/melt interface.

(III) $AlF_4^- + e = AlF_3^- + F^-$

(IV) $AlF_3^- + e = AlF_2^- + F^-$

(V) $AlF_2^- + e = Al + 2F^-$

(VI) Diffusion of 3NaF away from the metal/melt interface.

Steps III and IV may alternatively take place as a single step with a two-electron transfer. That AlF_2^- participates as an intermediate entity in the reaction scheme should be a logical consequence of its stability in the melt as discussed above. Any preceding reaction such as

$$AlF_4^- = Al^{3+} + 4F^-$$

is less likely to occur. The concentration of Al^{3+} must be extremely low, since this ion will exhibit a high coulombic force on the neighbouring F^- ions giving rise to strong Al–F bonds.

The direct route for producing sodium is given in Scheme 2.

Scheme 2:
(I) Migration of Na^+ to the cathode surface (1 Faraday).
(II) $Na^+ + e = Na(diss)$
(III) Diffusion of Na(diss) away from the cathode surface.

It should be noted that Na(diss) can be considered as a final cathode product produced on the cathode surface. The greater part of this product will participate as such in the so-called back reaction, while the rest will dissolve in the aluminium pool. The formation of sodium gas of atmospheric pressure on the cathode surface will only take place at high current densities [10, 11], or in basic melts with a high content of NaF [9].

The reaction steps proposed for the formation of one mole of $NaAlF_2$ is shown in Scheme 3.

Scheme 3:
(I) Migration of $2Na^+$ to the cathode surface (2 Faraday).
(II), (III) and (IV) As in Scheme 1.
(V) Diffusion of $NaAlF_2$ and NaF from the cathode surface.

Thonstad and Rolseth [10] found, from double pulse measurements, a charge transfer resistance of about 0.003 ohm cm^2 for the total cathode process, corresponding to exchange current densities of 36 and 18 A cm^{-2} for a one- and two-electron step reaction, respectively. Since both Na(diss) and aluminium are produced simultaneously by the cathode process it means that Reaction 1 establishes equilibrium concentrations on the cathode surface for external current densities less than the exchange current density. This important conclusion also agrees with the fact that the sodium content of aluminium increases with increasing cathodic current densities [1]. The sodium enrichment is caused by a shift in the melt composition at the cathode surface as discussed below.

Another conclusion to be drawn is that reaction Schemes 1 and 2 both take place simultaneously on the cathode surface. It is also expected that the overall reaction with the highest exchange current density will catalyse the other one. Suppose step II in Scheme 2 has the highest exchange current density. Then it follows that Na(diss) will be an electron donor (Na(diss) = $Na^+ + e$) for steps III, IV and V in Scheme 1 with the overall reaction

$$4Na(diss) + NaAlF_4 = Al + 4NaF$$

which is equivalent to Reaction 1. However, at present there is no experimental evidence showing which of the reaction schemes has the highest exchange current density.

Since there is little or no activation control of the cathode process, it follows that the overvoltage present must originate from the concentration gradients created by the diffusion steps described in Schemes 1–3. The concentration overvoltage referred to one single reference electrode will be of equal magnitude for all reaction schemes. It should be noted that the formation of Na(diss) (Scheme 2) does not create a shift in the NaF/AlF_3 ratio in the cathode boundary layer. Both Scheme 1 and 3 create a change in this ratio. However, as discussed below $NaAlF_2$ is partly transformed to Na(diss) in the boundary layer which means that the aluminium deposition reaction (Scheme 1) can be considered responsible for the whole shift in the NaF/AlF_3 ratio.

4. Concentration gradients in the boundary layers

When discussing concentration gradients we must distinguish between an open and a closed system. In the latter aluminium with unit activity reacts with the melt creating equilibrium concentrations as shown in Fig. 1, and there will be no concentration gradients. However, the NaF/AlF_3 activity ratio is slightly changed from its original value due to Reaction 1. This change increases with increasing concentration of Na(diss) or NaF in the melt. Then it follows that the activity/concentration relationship for the $NaF–AlF_3$ system will be somewhat different from the corresponding Al–NaF–AlF_3 system. However, the difference in the activities of NaF and AlF_3 in the two cases is believed to be of minor importance and will not be taken into account.

In an open system, as in industrial cells, the convective mass transfer in the bulk of the electrolyte is obviously very rapid. The greater part of the concentration gradients in laboratory cells will also be located at the Al/melt and at the melt/gas interfaces, as long as the crucible diameter is not too small and the interpolar distance not too high. Therefore, the mass transfer through the bulk melt will not be considered as a rate limiting step in the present work. Several types of concentration gradients will exist in an open Al–NaF–AlF_3 system. Some of these are discussed in the following.

4.1. *NaF/AlF_3 gradients. No external current*

Figure 2 illustrates concentration profiles in melts with three different compositions in contact with an aluminium phase. There is no external current and the surrounding phases do not react with the system. The situation should correspond to an open laboratory cell with inert linings and convective melt motion. The

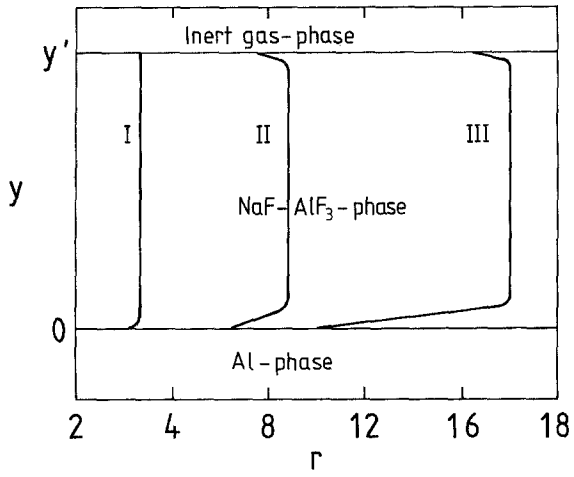

Fig. 2. Schematic concentration profiles expressed by the NaF/AlF_3 molar ratio r in an open Al–NaF–AlF_3 system for three different melt compositions (curves I, II and III) as a function of the distance y from the interface. The aluminium/melt interface is located at $y = 0$ while the melt/gas interface is at $y = y'$. No external current.

most important reactions taking place at the Al/melt interface will be

$$3NaF + Al \longrightarrow 3Na(diss) + AlF_3 \quad (1)$$

$$Na_3AlF_6 + 2Al \longrightarrow 3NaAlF_2 \quad (4)$$

$$NaF + NaAlF_2 \longrightarrow 2Na(diss) + AlF_3 \quad (5)$$

Reactions 1 and 4 are heterogeneous reactions taking place only at the metal/melt interface. Reaction 5 is a homogeneous reaction occurring throughout the boundary layer.

It is the continuous transport of reduced species away from the metal surface that establishes the concentration gradients of NaF and AlF_3 expressed by r as a single gradient in Fig. 2. It is important to note that Reaction 5 proceeds to the right in the diffusion layer next to the aluminium surface. The reason is that Na(diss) diffuses much faster than the other compounds, including $NaAlF_2$. This leads to the important conclusion that the melt composition at the Al/melt interface is more acidic than the bulk phase for all compositions, with a possible exception of melts close to saturation with AlF_3. Since Reaction 1 proceeds to the right at equilibrium the rapid diffusion of Na(diss) also means that the activity of aluminium gradually decreases from unity at the metal interface to a fixed value in the bulk phase. An aluminium electrode in an open NaF–AlF_3 system will then only be in equilibrium with the melt compositions on its surface and not with the bulk phase composition. One other conclusion is that factors affecting the fluxes, such as stirring, will make some minor changes in the melt composition adjacent to the metal surface and a corresponding small shift in the electrode potential should result. To the author's knowledge this point has so far not been studied experimentally.

In the boundary layer next to an inert gas phase the main reactions involving reduced entities are

$$Na(diss) \longrightarrow Na(g) \quad (6)$$

$$NaAlF_2 \longrightarrow NaF + AlF(g) \quad (7)$$

$$NaAlF_2 + NaF \longrightarrow 2Na(diss) + AlF_3 \quad (5)$$

Also, in this case, there is rapid transport of Na(diss), which means that Reaction 5 proceeds to the right in order to establish chemical equilibrium throughout the boundary layer. The shape of the NaF and AlF_3 gradients expressed by the concentration measure, r, is illustrated in Fig. 2. The equilibrium vapour pressure of Na(g) and AlF(g), the most important reduced entities in the gas phase, can be accurately interpolated from thermodynamic data for whatever composition in the Al–NaF–AlF_3 system and in the Al–NaF–AlF_3–Al_2O_3 system [4, 9]. In the acidic range of these systems it is also important to take into account the evaporation reactions

$$NaAlF_4 \longrightarrow NaAlF_4(g) \quad (8)$$

$$AlF_3 \longrightarrow AlF_3(g) \quad (9)$$

4.2. *NaF/AlF_3 gradients created by external current*

The NaF/AlF_3 gradient is affected by an external current since Na^+ is the carrier of current in the molten phase. An increasing cathodic current means that the concentration of NaF increases and that the concentration of AlF_3 decreases at the cathode surface. Some steady state concentration patterns are illustrated in Fig. 3.

By means of thermodynamic data for the NaF–AlF_3 system [4] at 1285 K it is easily calculated that sodium gas at 1 atm will be formed at a surface composition $r = 17.5$. The corresponding value for a melt saturated with alumina is $r = 10$ [9]. A gradual increase of the cathode current density finally gives sodium gas evolution resulting in mass transfer and current/voltage fluctuations as observed by Thonstad and Rolseth [10]. A further increase of the current increases mainly the sodium gas production.

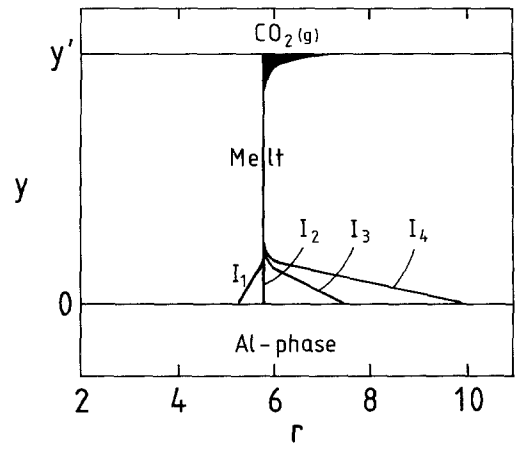

Fig. 3. Schematic concentration profiles described by the NaF/AlF_3 molar ratio r in an open Al–NaF–AlF_3 system as a function of the distance y from the aluminium/melt interface. Some arbitrary external steady state cathodic currents are presumed to be applied where $|I_4| > |I_3| > |I_2| > I_1 = 0$. y' is the total thickness of the salt phase. Oxidizing atmosphere.

It should be stressed that an oxidizing atmosphere, such as $CO_2(g)$, will shift the NaF/AlF_3 concentration gradient at the melt/gas interface in the direction opposite to that shown in Fig. 2. In basic melts the dominating reaction will be

$$6Na(diss) + 2AlF_3 + 3CO_2(diss) \longrightarrow Al_2O_3 + 6NaF + 3CO(g) \quad (10)$$

The net result is that the r value in the boundary layer adjacent to the gas phase increases, as indicated in Fig. 3, while alumina accumulates in the melt. Reaction 10 is discussed below.

Alumina will also be accumulated in highly acidic melts by direct oxidation of monovalent aluminium (AlF_2^-) together with a slow shift of the melt composition towards the basic side, as a consequence of the evaporation Reactions 8 and 9.

4.3. *Concentration gradients of reduced species*

From the above discussion it follows that the concentrations of the reduced entities Na(diss) and $NaAlF_2$ in the boundary layers are determined by the NaF/AlF_3 gradients through the equilibrium reaction

$$NaAlF_2 + NaF = 2Na(diss) + AlF_3 \quad (5)$$

Figure 4 illustrates concentration profiles of Na(diss) when the applied current is zero and at a certain cathodic current. The most important conclusion is that an increasing cathodic current increases both the NaF/AlF_3 ratio and the concentration of Na(diss) on the cathode surface. This conclusion is also supported by the fact that the sodium content of the aluminium cathode increases with increasing cathode current density [1].

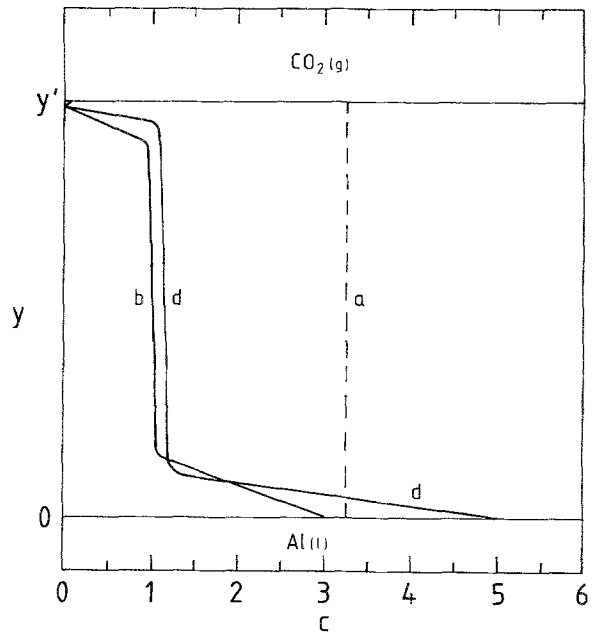

Fig. 4. Schematic concentration profiles of Na(diss) in the $NaF-AlF_3$–Al system. Both the concentration c and the distance y from the Al/melt interface are in arbitrary units. (a) Equilibrium concentration in the closed system. (b) Concentration profile in the open system with CO_2 atmosphere and no current. (d) Profile when the Al phase is made a cathode with a corresponding CO_2 evolution on the anode at y'.

The equilibrium concentration of $NaAlF_2$, referred to unit activity of aluminium, has a maximum value in a melt with the composition $r = 3.0$ as indicated in Figs 1 and 6. A steadily increasing cathodic current, which increases the NaF/AlF_3 ratio beyond $r = 3.0$ on the cathode surface, means that the surface concentration of $NaAlF_2$ passes through a maximum at $r = 3.0$. It is obvious that the concentration profiles for $NaAlF_2$ may be irregular.

The solubility of CO_2(diss) in the melt [12] is considerably lower than the total solubility of reduced species. Reaction 11

$$CO_2(g) = CO_2(diss) \quad (11)$$

can hardly be a rate limiting step in the overall oxidation reaction. Since the equilibrium concentration of CO_2(diss) is low, it means that the oxidation Reaction 10 must occur in the melt boundary layer at the gas/melt interface. The net effect of an oxidizing atmosphere, compared to an inert one, will be a slightly reduced concentration level of the reduced species in the bulk phase and a corresponding increase in the total flux of reduced entities. This effect may be hard to detect experimentally, if the convection is high in the bulk phase of the melt.

Most workers [1] have found that the rate of the overall reoxidation reaction is, within experimental uncertainty, independent of the pressure ratio CO_2/CO, which clearly shows that Reaction 10 is rapid and does not represent a rate limiting step in the overall recombination process.

Thus there should be no doubt that the Na(diss) concentration profile b in Fig. 4 is generally correct. It is also reasonable to believe that the thickness of the liquid boundary layer adjacent to the gas/melt interface is somewhat less than the thickness of the corresponding layer at the melt/metal interface. This will especially be the case when gas bubbles escape the melt surface, disrupting the boundary layer. The effective surface area also increases, as Reaction 10 also takes place in the boundary layer around the CO_2 gas bubbles. The convection such bubbles create may reduce the thickness of the cathode boundary layer. However, the reduction of the thickness of the melt/gas boundary layer is even more extensive. Hence, the rate of the metal loss processes during electrolysis in technical cells is expected to be mostly controlled by mass transfer through the boundary layer next to the metal surface. This conclusion is in agreement with a recent study of Solheim and Thonstad [13] who found that the melt/gas interface accounts for less than 10% of the transport resistance of dissolved metal. In laboratory cells the situation is sometimes different since the ratio of cross sectional area of the two boundary layers may vary within wide limits depending on the experimental conditions. In this respect the rounded shape of the metal surface should be considered.

Another point to be discussed below is the fact that the diffusion layer thickness will be different for dif-

ferent types of compounds. The diffusion layer thickness of the electronic conducting compound Na(diss) is much smaller than that for typical ionic compounds.

Since Reaction 5 proceeds to the right in the diffusion layer it means that the rate of diffusion of reduced species will be greatly enhanced. It also means that the boundary layer thickness of $NaAlF_2$ will be reduced to a small value. However, at present, the lack of data do not allow a precise calculation of the exact shape of the concentration profiles.

5. Current for Al deposition and concentration gradients

So far the NaF and AlF_3 gradients have been expressed as a single gradient using the molar ratio r as a concentration measure. This means that they are intimately interlinked by the flux equation (Scheme 1)

$$J_{NaF} = -3J_{AlF_3} \quad (12)$$

valid under steady state conditions and considered independent of CE. It follows that the average partial current density, i_{Al}, related to the flux densities at the electrode–solution interface,

$$i_{Al} = -3FJ_{AlF_3} = FJ_{NaF} \quad (13)$$

has a negative sign at zero and small external cathodic current densities (see Fig. 3). At higher cathodic currents i_{Al} acquires a positive sign corresponding to a shift in the mass flow direction of both NaF and AlF_3 as illustrated in Fig. 3. The turning point corresponds to the situation that the aluminium loss, described by Schemes 2 and 3, is compensated by the aluminium production.

In a binary non-ideal system Fick's law may be rewritten in the form

$$J_{NaF} = -c_{NaF}D_{NaF}\left[\frac{\mathrm{d}\ln a_{NaF}}{\mathrm{d}y}\right]_{y=0} \quad (14)$$

where y is normal to the aluminium/melt interface and directed into the solution. Equation 14 may be written as

$$J_{NaF} = -D_{NaF}\frac{x}{V}\left[\frac{\mathrm{d}\ln a_{NaF}}{\mathrm{d}y}\right]_{y=0} \quad (15)$$

where x is the molar fraction of NaF and V is the integral molar volume.

From Fig. 5 it follows that the activity of NaF [4] can tentatively be expressed by the empirical equation

$$\ln a_{NaF} = -A'(x - 0.25)^{-1} + B' \quad (16)$$

where A' and B' can be linearized with respect to temperature

$$A' = -0.00325T + 6.320 \quad (17)$$

$$B' = -0.006425T + 11.450 \quad (18)$$

Equations 16–18 give activity data in fair agreement with thermodynamic data presented elsewhere [4]. Derivation of Equation 16 at a certain temperature,

$$\mathrm{d}\ln a_{NaF} = A'(x - 0.25)^{-2}\mathrm{d}x \quad (19)$$

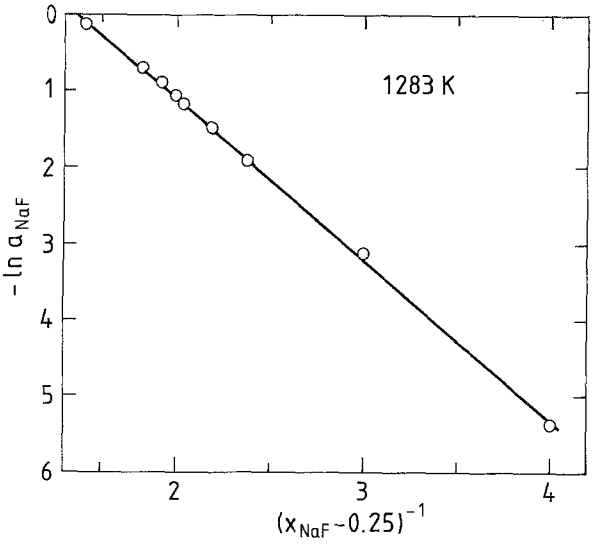

Fig. 5. Log of NaF activity in the system NaF–AlF_3 as a function of $(x_{NaF} - 0.25)^{-1}$, where x_{NaF} is the molar fraction of NaF. Temperature 1283 K.

and combination with Equations 13 and 15 yield

$$i_{Al}\mathrm{d}y = -FD_{NaF}\frac{xA'}{V(x - 0.25)^2}\mathrm{d}x \quad (20)$$

The integral molar volume V is a function of both composition and temperature. Values for V at 1283 K calculated from density data of Paucirova *et al.* [8] are given in Table 1 at various melt compositions. The next step is to simplify Equation 20. Empirically it is found that

$$\frac{xA'}{V(x - 0.25)^2} \simeq \frac{A''}{(x - 0.35)^{0.555}} \quad (21)$$

where

$$A''(\mathrm{mol\,cm^{-3}}) = 0.458 - 0.306T/T_0 \quad (22)$$

with $T_0 = 1273$ K. Numerical values for these expressions are included in Table 1 showing that the mutual fit is fairly good for an arbitrary temperature of 1283 K. Combination of Equations 20 and 21 gives

$$i_{Al}\mathrm{d}y = -FD_{NaF}A''(x - 0.35)^{-0.555}\mathrm{d}x \quad (23)$$

Equation 23 is then integrated over the Nernst dif-

Table 1. The second column shows values for the integral molar volume, V, calculated from density data [8] at various molar fractions of NaF, x. The next two columns show that Equation 21 (see text) is satisfied reasonably well. A′ = 2.15 and A″ = 0.152. Temperature 1283 K

x	V ($cm^3\,mol^{-1}$)	$\frac{xA'}{V(x - 0.25)^2}$	$\frac{A''}{(x - 0.35)^{0.555}}$
0.80	24.06	0.236	0.236
0.77	24.60	0.249	0.246
0.75	25.06	0.257	0.253
0.70	26.70	0.278	0.272
0.65	28.78	0.303	0.297
0.60	31.78	0.331	0.328
0.55	35.51	0.370	0.371
0.50	39.00	0.441	0.436

fusion layer thickness δ yielding

$$i_{Al} = \frac{FA''k_{NaF}}{0.445}[(x^* - 0.35)^{0.445} - (x - 0.35)^{0.445}] \quad (24)$$

where $k_{NaF} = D_{NaF}/\delta_{NaF}$ is the mass transfer coefficient of NaF, while x^* is the molar fraction of NaF at the aluminium surface and x is the corresponding bulk concentration. The integration is based on the assumption of a concentration independent diffusion coefficient in the range from x^* to x.

6. Overvoltage and concentration gradients

The overvoltage should, if possible, be referred to a single electrode reaction. As discussed in the preceding section several reactions take place at the aluminium/melt interface, creating concentration gradients which give rise to concentration overvoltage. According to the IUPAC conventions [14] the concentration overvoltage can be described by the open circuit potential of a concentration cell where both electrodes are equilibrated to the same single electrode reaction. We may tentatively write the cell,

$$Al|NaF, AlF_3 \| NaF, AlF_3|Al \quad (25)$$

where the left hand side compartment corresponds to the bulk concentration and the right hand side to the interface concentrations of the working electrode. The transport properties of the junction should be equal to those existing in the diffusion layer creating overvoltage. Since the transport number of Na^+ is taken to be unity in the whole range studied $1 < r < 10$, the hypothetical open circuit potential equal to the concentration overvoltage can be expressed by the equation

$$\eta_{Al} = \frac{RT}{F}\ln\frac{a_{NaF}}{a_{NaF^*}} + \frac{RT}{3F}\ln\frac{a_{AlF_3^*}}{a_{AlF_3}} \quad (26)$$

where * denotes activities in the right hand side compartment. It should be emphasized that cell 25 must be referred to a closed system with no concentration gradients in the cell compartments. Measured potentials of cell 25 in an open system [11] correspond approximately with Equation 26 in acidic melts while there are considerable deviations in the basic range of the system [9]. As discussed above the main reason for this deviation is that the aluminium electrode in an open system does not behave reversibly with respect to the bulk concentrations. Nevertheless Equation 26 is still the most convenient and precise definition of the concentration overpotential for the reduction of trivalent aluminium ions using activities referred to the bulk phase composition.

There are several alternative ways of expressing the concentration overpotential as a function of composition. If we introduce the expressions for the activity of AlF_3 from the following equilibria

$$AlF_3 + NaF = NaAlF_4 \quad (27)$$

$$AlF_3 + 3NaF = Na_3AlF_6 \quad (28)$$

Table 2. Concentration overvoltage in NaF–AlF_3 melts calculated from Equations 26 and 32 (see text) for various molar fractions of NaF. Activity data from Sterten et al. *[4]. r is the NaF/AlF_3 molar ratio. Reference melt r = 1.0 corresponds to zero overvoltage*

r	x_{NaF^*}	η_{Al} (V) (Equation 26)	η_{Al} (V) (Equation 32)
1.0	0.500	0.000	0.000
1.4	0.583	−0.340	−0.326
1.8	0.643	−0.493	−0.493
2.4	0.706	−0.634	−0.637
3.0	0.750	−0.718	−0.723
4.0	0.800	−0.809	−0.809
10.0	0.909	−0.992	−0.969

in the equation for the overvoltage, Equation 26, the result will be

$$\eta_{Al} = \frac{4RT}{3F}\ln\frac{a_{NaF}}{a_{NaF^*}} + \frac{RT}{3F}\ln\frac{a_{NaAlF_4^*}}{a_{NaAlF_4}} \quad (29)$$

$$\eta_{Al} = \frac{2RT}{F}\ln\frac{a_{NaF}}{a_{NaF^*}} + \frac{RT}{3F}\ln\frac{a_{Na_3AlF_6^*}}{a_{Na_3AlF_6}} \quad (30)$$

Equations 29 and 30 can also be combined to give

$$\eta_{Al} = \frac{RT}{F}\ln\frac{a_{NaAlF_4^*}}{a_{NaAlF_4}} + \frac{2RT}{3F}\ln\frac{a_{Na_3AlF_6}}{a_{Na_3AlF_6^*}} \quad (31)$$

It is immaterial which of the Equations 26, 29–31 is used to derive numerical values for the overvoltage as long as interconsistent activity data are employed [4].

In the following treatment activity data of the binary NaF–AlF_3 system are applied to calculate the overpotential at various interface concentrations referred to the bulk concentration $r = 1.0$. These numerical values given in Table 2 were used to derive an empirical equation describing the relationship between the overvoltage and the interface molar ratio of NaF as follows

$$\eta_{Al} = B'' + B\ln(x^* - 0.35) \quad (32)$$

where $B'' = -1.397$ V and $B = -0.736$ V.

The results in Table 2 show that Equation 32 does not deviate seriously from the more fundamental Equation 26. Equation 32 may be transformed to a more general and applicable form

$$\eta_{Al} = B\ln\left[\frac{x^* - 0.35}{x - 0.35}\right] \quad (33)$$

Table 3. Concentration overvoltage, $\eta = A_l + B_l$ in NaF–AlF_3 melts at 1285 K. $A_l = (RT/F)\ln(a_{NaF}/a_{NaF^*})$ and $B_l = (RT/3F)\ln(a_{AlF_3^*}/a_{AlF_3})$ is the overvoltage contribution from the gradients of NaF and AlF_3, respectively. The reference melt is the NaF/AlF_3 molar ratio r = 2.4. Activity data are taken from the work of Sterten and Mæland [4]

r	A (V)	B (V)
2.4	0.000	0.000
2.6	−0.015	−0.011
2.8	−0.033	−0.023
3.0	−0.047	−0.036
3.4	−0.067	−0.061
3.7	−0.079	−0.075
4.0	−0.087	−0.086

where x as usual denotes the bulk molar fraction of NaF. A certain concentration gradient corresponds to a certain overpotential independent of temperature.

Table 3 shows that the NaF and the AlF_3 gradients, as expressed by Equation 26, create an overvoltage of roughly equal magnitude in the range $2.4 < r < 4$. Outside these limits the contribution to the overvoltage from each gradient is not of the same size.

7. Overvoltage and current for aluminium deposition

In order to derive the relationship between the overpotential and the partial current density of aluminium, we need to combine Equations 24 and 33. Rearrangement of Equation 33 yields

$$(x^* - 0.35) = (x - 0.35)\exp(\eta_{Al}/B) \quad (34)$$

from which it follows

$$(x^* - 0.35)^{0.445} = (x - 0.35)^{0.445}\exp(0.445\eta_{Al}/B) \quad (35)$$

Why 0.445 is applied as an exponent is easily seen when Equation 35 is combined with Equation 24 to give,

$$i_{Al} + \frac{Fk_{NaF}A''}{0.445}(x - 0.35)^{0.445} = \frac{Fk_{NaF}A''}{0.445}(x - 0.35)^{0.445}\exp(0.445\eta_{Al}/B) \quad (36)$$

Introducing the term

$$a = \frac{Fk_{NaF}A''}{0.445}(x - 0.35)^{0.445} \quad (37)$$

in Equation 36 and rearranging gives the required relationship between overvoltage and current density.

$$\eta_{Al} = 1.654 \ln\left[\frac{a}{i_{Al} + a}\right] \quad (38)$$

The temperature dependence of A'' should be noted, Equation 22.

8. Overvoltage and current loss

The greater part of the loss in CE can be ascribed to the total mass transfer of reduced species through the cathode boundary layer. The equilibrium concentrations of Na(diss) and $NaAlF_2$ referred to a closed system are shown in Fig. 6. As discussed above there is a rapid transformation of monovalent aluminium compounds to Na(diss) in the boundary layer as described by Reaction 5. The net result will be that the slope of the concentration profiles for $NaAlF_2$ and Na(diss) may approach each other. In such a case it is obviously convenient to define the total flux of reduced species, J_{loss}, by the driving force of only one of the components. We may tentatively write

$$J_{loss} = \frac{i_{loss}}{F} = k_{Na}(c^*_{Na} - c_{Na,b}) \quad (39)$$

where c_{Na^*} and $c_{Na,b}$ are the concentrations of Na(diss)

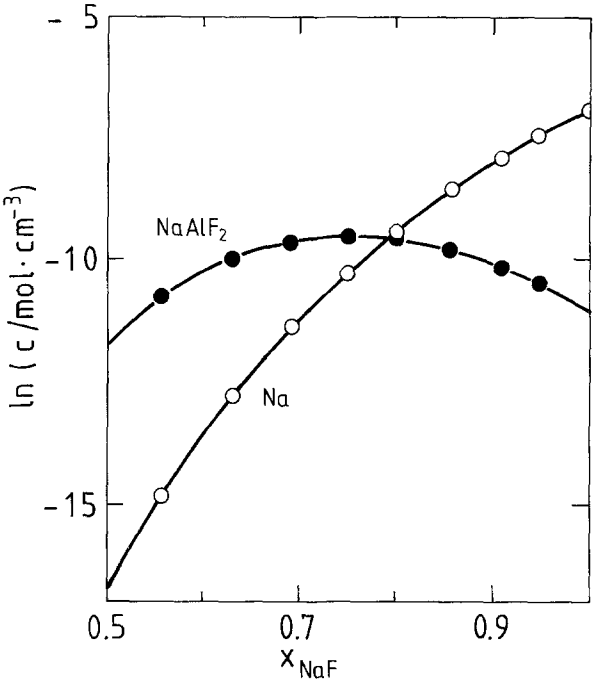

Fig. 6. Log of the concentrations of the reduced species Na(diss) and $NaAlF_2$ as a function of the molar fraction x_{NaF} in the closed Al–NaF–AlF_3 system at 1273 K.

at the aluminium surface and in the bulk phase, respectively. k_{Na} is a mixed mass transfer coefficient for all reduced species. A possible variation of k_{Na} with interfacial and bulk concentrations should not be excluded. However, as discussed below, this variation seems to be small.

The concentration of Na(diss) in the bulk phase of an open system, $c_{Na,b}$, will only be a fraction, α, of the corresponding equilibrium concentration in the closed system, $c_{Na,eq}$, as indicated in Fig. 4.

$$c_{Na,b} = \alpha c_{Na,eq} \qquad 0 < \alpha < 1 \quad (40)$$

Combining Equations 39 and 40 and solving for the interface concentration yields

$$c_{Na^*} = \frac{i_{loss}}{Fk_{Na}} + \alpha c_{Na,eq} \quad (41)$$

Equation 26, describing the concentration overvoltage for aluminium deposition, can be combined with the equilibrium Reaction 1 as follows

$$\eta_{Al} = \frac{RT}{F}\ln(c_{Na,eq}/c_{Na^*}) \quad (42)$$

From Equations 41 and 42 one obtains

$$\eta_{Al} = -\frac{RT}{F}\ln\left[\frac{i_{loss} + k\alpha}{k}\right] \quad (43)$$

where

$$k = Fk_{Na}c_{Na,eq} \quad (44)$$

Equation 39 should probably be rewritten with some other driving force for highly acidic melts, since it is to be expected that k_{Na} will be dependent on composition in that part of the system. It may be proposed that the total solubility expressed as wt % Al should be used as the driving force for the back reaction. However, the

relationships between overvoltage and metal solubility/current loss are not easily derived in that case.

9. Cathodic current efficiency

The next step is to solve Equation 43 with respect to i_{loss} and introduce the term given in Equation 44,

$$i_{loss} = Fk_{Na}c_{Na,eq}\left[-\alpha + \exp\left(-\frac{F}{RT}\eta_{Al}\right)\right] \quad (45)$$

From the Equations 22, 37 and 38 we obtain

$$i_{Al} = Fk_{NaF}c_m[-1 + \exp(0.445\eta_{Al}/B)] \quad (46)$$

where

$$c_m(\text{mol cm}^{-3}) = (1.030 - 0.687T/T_0) \times (x - 0.35)^{0.445} \quad (47)$$

with $B = -0.736$ V and $T_0 = 1273$ K. c_m can be considered as a modified concentration of NaF. The variation of c_m with composition should correspond to the variation of the 'effective' NaF concentration.

It should be noted that i_{Al} and i_{loss} are local current densities at a given point on the surface of the metal.

Equation 45 does not describe the total loss in an aluminium reduction cell. Reoxidation of dispersed metal in the salt phase should be taken into account when analysing CE. Cathodic reduction of impurities reduces the current yield of aluminium somewhat. Some aluminium carbide is also formed by reaction of the metal with the carbon bottom of the cell. Sodium penetration into the carbon cathode will also take place to a certain degree. The current efficiency, ε_{Al}, with respect to aluminium formation/dissolution may then be written

$$\varepsilon_{Al} = [i_{Al}/(i_{Al} + i_{loss})] - \varepsilon'_{Al} \quad (48)$$

where ε'_{Al} represents the unspecified losses indicated above.

10. Comparison of theory with experimental data

Equations 45–48 should be tested against experimental data. Thus we need data for cathodic overvoltage and current efficiency as a function of current density from cells where ε'_{Al}, the unspecified losses in Equation 48, can be estimated or neglected. Of special interest is to test the variation of the mass transfer or the proportionality constant k_{NaF} and k_{Na} with respect to the cathodic current density. The thicknesses of the diffusion layers depend critically on the flow rate of electrolyte along the cathode surface, and may be influenced by the rate of the anode gas evolution, especially at short interelectrode distances. There is a lack of consistent literature data so that a critical evaluation of model parameters is at present not possible. The importance of cathodic overvoltage has not been given sufficient attention in conjunctions with current efficiency determinations. However, in the literature there is one work that systematically describes cathodic overvoltage as a function of current density and melt composition. Some sets of data from this work of Thonstad and Rolseth [10, 11] will be analysed in some detail.

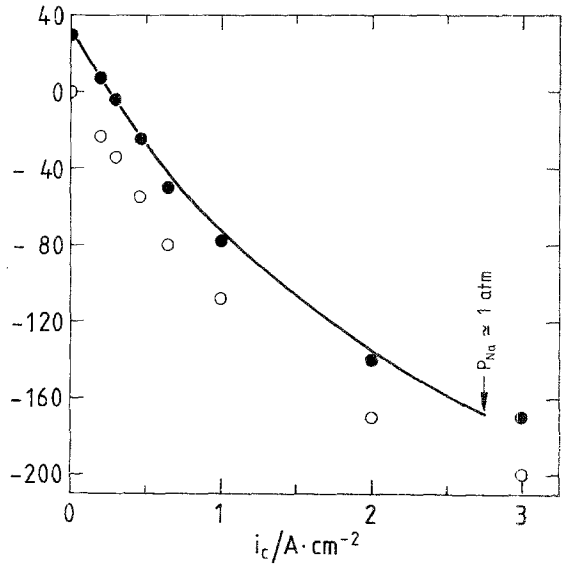

Fig. 7. Overvoltage as a function of total current density at the aluminium cathode in an open Al–NaF–AlF_3–Al_2O_3(sat) system at 1273 K. Melt composition $r = 4$ (NaF/AlF_3 molar ratio). Open circles from Thonstad and Rolseth [10] are displaced 30 mV (filled circles). The curve is calculated (see text).

10.1. *Overvoltage and current density*

We tried to fit overvoltage/current density data of Thonstad and Rolseth [10] to the Equations 45–48 assuming $\varepsilon'_{Al} = 0$. It turned out to be difficult to assess the optimum parameter fit because of too many unknown variables. However, good fits to experimental data were easily obtained as illustrated in Fig. 7. The curve drawn in the figure indicates that the NaF/AlF_3 gradient at the aluminium electrode corresponds to about 30 mV when the external current is zero. Therefore, all the experimental points in the figure (open

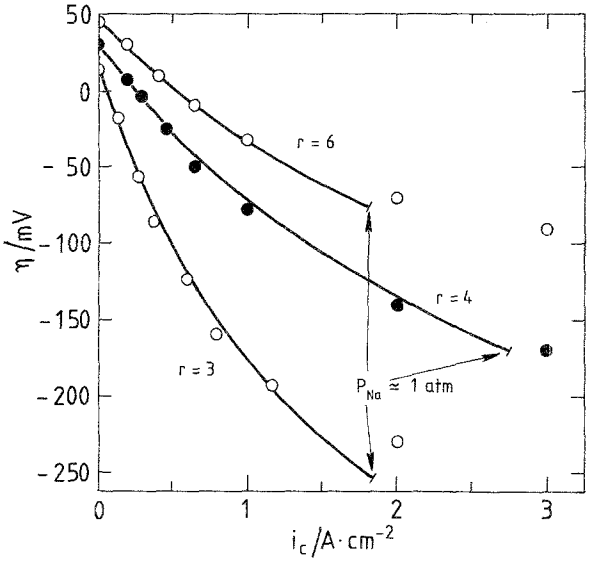

Fig. 8. Overvoltage as a function of total current density at the aluminium cathode in an open Al–NaF–AlF_3–Al_2O_3(sat) system at 1273 K. The melt compositions are expressed by r the NaF/AlF_3 molar ratio. Experimental points are from Thonstad and Rolseth [10], while the curves are calculated from the present work (see text).

Table 4. Numerical values of the mass transfer coefficients k_{NaF} *and* k_{Na} *used to calculate the curves shown in Fig. 8.* α *is the degree of saturation of Na(diss) in the bulk phase, while* r *is the NaF/AlF*$_3$ *molar ratio of the melt*

r	α	k_{NaF} ($cm\,s^{-1}$)	k_{Na} ($cm\,s^{-1}$)
3.0	0.50	2.2×10^{-4}	0.033
4.0	0.50	3.0×10^{-4}	0.065
6.0	0.50	2.5×10^{-4}	0.060

circles) have been displaced upwards by 30 mV (filled circles).

Increasing the cathodic current density from zero changes the NaF/AlF_3 gradient to zero at $i_c \simeq 0.24\,A\,cm^2$ as may be seen from Fig. 7. At higher cathodic current densities a net production of aluminium will take place while the NaF/AlF_3 gradient develops in the opposite direction of the gradient at low current densities.

The curve shown in Fig. 7 is also included in Fig. 8 together with similar curves obtained for other melt compositions. We see that there is a good fit between the experimental points of Thonstad and Rolseth [10] and the calculated curves. The parameters used in the calculations are summarized in Table 4.

Figure 9 shows the relationship between overvoltage and the partial current densities of i_{Al} and i_{loss} for $r = 3$. The relative increase of sodium production with increasing current densities should be noted. Figure 10 shows the corresponding CE. Although the magnitude of CE is uncertain, the shape of the curve in Fig. 10 is in general agreement with experimental data [16].

11. Discussion

All the overvoltage data of Thonstad and Rolseth

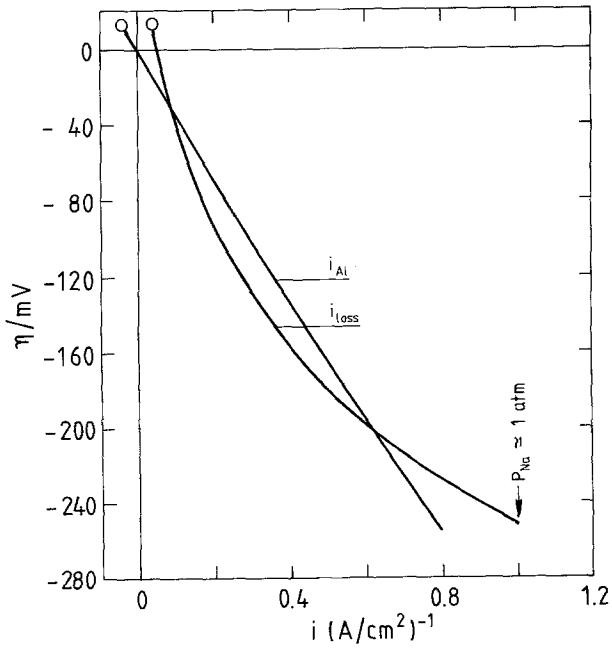

Fig. 9. Overvoltage as a function of the partial current densities, i_{Al} and i_{loss} at 1273 K (see text). Melt composition $r = 3$ (NaF/AlF_3 molar ratio).

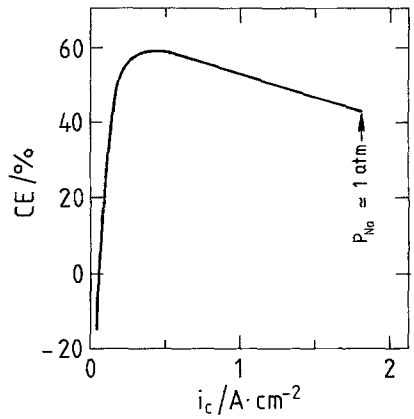

Fig. 10. Calculated current yield of aluminium from the data shown in Fig. 9 as a function of the total current density.

described above were obtained in a graphite crucible, the wall of which served as the anode. Two identical aluminium electrodes housed in sintered alumina cups of 16 mm i.d. were used as working electrode and reference electrode, respectively. Such a cell arrangement gives unusually low anodic current densities and the corresponding gas evolution on the crucible wall would only have a negligible effect on the boundary layer next to the aluminium surface. This surface was usually located 2–4 mm below the rim of the alumina cup [11] giving rise to a rather high thickness of the boundary layer. It should also be stressed that the shape of the cathode surface was nearly hemispherical giving rise to a non-uniform current distribution. The current density data of Thonstad and Rolseth [10] were referred to the cross-sectional area of the cup housing the metal, which means that these data are considerably higher than the average current densities.

The results given indicate that the parameters k_{NaF}, k_{Na} and α may be independent of the electrode overvoltage and the current density. However, this important implication should be studied more thoroughly, especially the expected variation of k_{Na} in extremely acidic melts. The low value of $k_{NaF} \simeq 2.5 \times 10^{-4}\,cm\,s^{-1}$ obtained should be noted. Such a value corresponds to a Nernst diffusion layer thickness in the range $0.1\,cm < \delta_{NaF} < 0.3\,cm$ which should be regarded as a reasonable value, when considering the shielding effect of the alumina cup housing the aluminium electrode.

On the other hand the values for k_{Na} in Table 4 are extremely high. These results support the idea of 'electronic' conduction of Na(diss) and mass transfer via a chemical reaction in the cathode boundary layer. The high values for k_{Na} also indicate that the thicknesses of the boundary layers of reduced species must be considerably smaller than the corresponding thickness of the NaF layer. This proposition leads to the interesting conclusion that k_{Na} is less affected than k_{NaF} by convection. Since the forced convection in industrial cells is higher than the natural convection in laboratory cells it means that the CE in industrial cells should be higher than in laboratory cells at high enough current densities. This conclusion is in general agreement with what is observed. However, the term ε'_{Al} in Equation

48 may become increasingly important with increased convection. There is reason to believe that there are rather large local variations in the magnitude of the mass transfer coefficients at the cathode surface in industrial cells. The influence of various parameters, such as magnetic field and interfacial tension, on the mass transfer coefficients should be investigated in order to obtain an improved understanding of the cathode process.

References

[1] K. Grjotheim, C. Krohn, M. Malinovsky, K. Matiasovsky and J. Thonstad, 'Aluminium Electrolysis. Fundamentals of the Hall–Heroult Process', 2nd edn, Aluminium-Verlag, Düsseldorf (1982).

[2] K. Grjotheim, W. E. Haupin and B. J. Welch, 'Light Metals' (edited by H. O. Bohner), Proc. of 114th Annual Meeting, New York (1985) pp. 679–694.

[3] R. Ødegård, On the solubility and electrochemical behaviour of aluminium and aluminium carbide in cryolitic melts, Thesis, Univ. of Trondheim, NTH, Trondheim, Norway (1986).

[4] Å. Sterten and I. Mæland, *Acta Chem. Scand.* **A39** (1985) 241.

[5] K. S. Pitzer, *J. Am. Chem. Soc.* **84** (1962) 2025.

[6] M. A. Bredig and H. R. Bronstein, *J. Phys. Chem.* **64** (1960) 64.

[7] M. A. Bredig, in 'Molten Salt Chemistry' (edited by M. Blander), Interscience, New York (1964).

[8] M. Paucirova, K. Matiasovsky and M. Malinovsky, *Rev. Roumaine Chim.* **15** (1970) 33.

[9] Å. Sterten, K. Hamberg and I. Mæland, *Acta Chem. Scand.* **A36** (1982) 329.

[10] J. Thonstad and S. Rolseth, *Electrochim. Acta* **23** (1978) 221.

[11] *Idem, ibid.* **23** (1978) 233.

[12] D. Bratland, K. Grjotheim, C. Krohn and K. Motzfeldt, *J. Metals* **19** (1967) 13.

[13] A. Solheim and J. Thonstad, 'Light Metals' (edited by R. D. Zabreznik), Proc. of 116th AIME Annual Meeting, Denver, Colorado (1987) pp. 239–245.

[14] N. Ibl, *Pure Appl. Chem.* **53** (1981) 1827.

[15] S. Rolseth and J. Thonstad, 'Light Metals' (edited by G. M. Bell), Proc. of 110th AIME Annual Meeting, Chicago (1981) pp. 289–301.

[16] Å. Sterten, S. Rolseth, E. Skybakmoen, A. Solheim and J. Thonstad, 'Light Metals' (edited by L. G. Boxall), Proc. of 117th AIME Annual Meeting, Phoenix, Arizona (1988) pp. 663–670.